

## Power-Law Spatial Correlations in Arrays of Locally Coupled Lasers

Fabien Rogister,<sup>1,\*</sup> K. Scott Thornburg, Jr.,<sup>2</sup> L. Fabiny,<sup>2</sup> Michael Möller,<sup>3</sup> and Rajarshi Roy<sup>4</sup>

<sup>1</sup>*Service d'Electromagnétisme et de Télécommunications, Faculté Polytechnique de Mons, Boulevard Dolez 31, 7000 Mons, Belgium*

<sup>2</sup>*School of Physics, Georgia Institute of Technology, Atlanta, Georgia 30332, USA*

<sup>3</sup>*Institut für Angewandte Physik, Westfälische Wilhelms-Universität Münster, D-48149 Münster, Germany*

<sup>4</sup>*Institute for Physical Science and Technology and Department of Physics, University of Maryland, College Park, Maryland 20742, USA*

(Received 18 September 2003; published 5 March 2004)

We investigate correlations of the intensity fluctuations of two-dimensional arrays of nonidentical, locally coupled lasers, numerically and experimentally. We find evidence of a power-law dependence of spatial correlations as a function of laser pair distance (or coupling strength) near the phase-locking threshold.

DOI: 10.1103/PhysRevLett.92.093905

PACS numbers: 42.65.Sf, 05.45.Xt

The study of large populations of interacting elementary oscillators, systems likely to display self-organization and spatiotemporal chaos, has relevance in many areas of science ([1,2] and references therein). Revealing universal principles underlying the emergence of coherence in systems that differ in the intrinsic dynamics of their individual elements and the coupling topology is an important issue. One generally discerns three different kinds of coupling: local coupling where each element interacts only with its direct neighbors, global coupling where each element interacts with all the others, and nonlocal coupling, which is the intermediate case. Global coupling was demonstrated by Winfree [3] and Kuramoto [4] to induce a cooperative phenomenon, analogous to a phase transition, in the case of infinite sets of limit-cycle oscillators with different frequencies. Very recently, Kiss and co-workers quantitatively tested this theory successfully with an electrochemical system [5]. In addition, they found qualitatively similar results when the oscillators operate in chaotic regimes. In the case of large sets of perfectly identical but nonlocally coupled periodic and chaotic oscillators, Kuramoto and Nakao gave evidence that spatial correlations decay with a power law on length scales smaller than the range of coupling [6,7]. As far as we are aware, this behavior has not yet been reported in an experiment.

Laser arrays are excellent examples of coupled nonlinear oscillators; they are experimentally realizable systems in which the coupling strength between elements can be tuned over several orders of magnitude. Phase transitions similar to those studied in Refs. [3,4] have been numerically predicted in the case of globally coupled lasers [8–10]. In contrast, power-law spatial correlations have been neither predicted nor experimentally observed in laser arrays.

The results of experiments and numerical simulations presented in this Letter are devoted to the study of the power-law dependence of the spatial correlations in arrays of nonidentical, locally coupled, chaotic lasers. We first report experiments on a two-dimensional square

array of nine lasers where each element is coupled to its nearest neighbors via feedback from an intracavity element. A power-law dependence of the spatial cross-correlation coefficients as a function of relative pair distance is experimentally observed. In a second step, we numerically investigate a model of this system and show that it reproduces the experimental observations. In order to minimize the edge effects inherent to a small array and to substantiate our results, we finally investigate the behavior of a much larger array and numerically demonstrate a progressive emergence of coherence and a very clear power-law dependence of the spatial correlations as a function of the local coupling strength. These new results are of general interest and provide evidence of power-law spatial correlations in an experimental system. In addition, we show that this behavior is not restricted to large sets of identical, nonlocally coupled oscillators but occurs also with arrays of nonidentical, locally coupled oscillators, and that the power law extends over a spatial range much larger than the coupling.

Figure 1 presents schematically the experimental setup. A Dammann holographic grating creates a two-dimensional square array of nine ( $3 \times 3$ ) distinct pump beams with nearly equal powers from a single incident beam emitted by an Ar<sup>+</sup> laser ( $\lambda = 514.5$  nm).

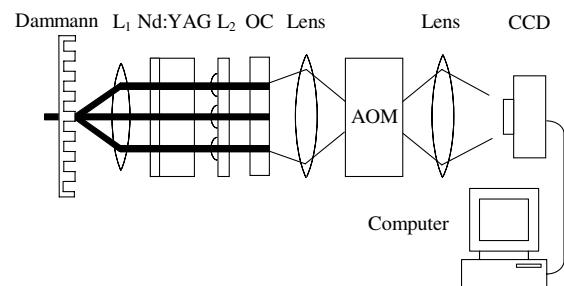


FIG. 1. Experimental setup. The Nd:YAG (neodymium doped yttrium aluminum garnet) crystal is pumped by nine beams from an argon laser. The intensities of the nine lasers are recorded simultaneously by the charge coupled device camera.

The period of the Dammann grating is  $158.9 \mu\text{m}$  leading to an angular separation between the diffracted beams of  $3.24 \text{ mrad}$ . The grating is located at the focus of a lens ( $L_1$ ,  $240 \text{ mm}$  focal length) such that, after passing through the lens, the nine beams propagate parallel to the optic axis with a separation of  $768 \mu\text{m}$ , and their waist is located inside a Nd:YAG crystal ( $5 \text{ mm}$  long,  $5 \text{ mm}$  diameter). Each pump beam generates an infrared laser beam lasing at  $1064 \text{ nm}$ . The resonator (about  $15 \text{ mm}$  long) is constituted on one side by the external facet of the crystal that is high-reflection coated and, on the other side, by a  $2\%$  transmissive output coupler (OC). A micro-lens array ( $L_2$ , focal length  $8.6 \text{ cm}$ ) is inserted within the resonator. The center-to-center spacing of the lens array is equal to the distance between the beams for proper beam overlap with all of the laser cavity spatial modes. The convex surfaces of the lenses are not antireflection coated, while the other side is. Because each beam expands as it propagates, and because of the Fresnel reflection (about  $4\%$  of the incident power) on the convex surface of the lenses, the effective area of the feedback beams is substantially larger (about  $40\%$ ) on return than the original beams. This enlargement provides coupling between array elements. The coupling is local to a good approximation as its strength decreases exponentially with the laser separation. By contrast, there is no appreciable coupling between the laser inversions inside the crystal as the pump beams have  $1/e^2$  beam radii of about  $20 \mu\text{m}$ , which is negligible in comparison with the laser separation. The intensities of the nine lasers are recorded simultaneously by using a charge coupled device (CCD) camera. An acousto-optic modulator (AOM) is used as an electronically controlled variable-time shutter.

While the lasers are stable when they are separate, they are driven completely unstable in the presence of the coupling [11]; the individual intensities, but also the total intensity, show large fluctuations. In addition, the linewidth of a single laser is measured to be larger than  $3 \text{ GHz}$ , as opposed to less than  $20 \text{ MHz}$  for a single longitudinal mode in the absence of coupling of the laser element with its neighbors. In order to quantify the degree of correlation between the elements of the array, we compute the ensemble-averaged spatial cross-correlation coefficients  $\langle \Gamma_i \rangle$ . We define the spatial cross-correlation coefficients  $\Gamma_i$  as

$$\Gamma_i = \frac{\sum_{j,k \in \{i\}}^{M_i} C_{j,k}}{M_i}, \quad (1)$$

where the sum is taken over all  $M_i$  pairs of lasers  $j$  and  $k$  whose distance is  $D_i$ . In Eq. (1),  $C_{j,k}$  is the cross-correlation coefficient between the intensities of the optical fields emitted by lasers  $j$  and  $k$ , i.e., the ratio of the covariance between the two intensities to the product of the standard deviations of the respective intensities. If the distance between nearest-neighbor pairs is taken to be  $d_{\text{n.n.}}$ , the only possible relative distances between laser

pairs in the  $3 \times 3$  array and the corresponding number of pairs are  $D_i/d_{\text{n.n.}} = 1, \sqrt{2}, 2, \sqrt{5}$ , and  $\sqrt{8}$ , and  $12, 8, 6, 8$ , and  $2$ , respectively. The ensemble averaging is then achieved by computing the average value of these quantities over 20 realizations. Figure 2 presents the ensemble-averaged cross-correlation coefficients  $\langle \Gamma_i \rangle$  as a function of pair distances ( $D_i/d_{\text{n.n.}}$ ) for three slightly different microlens tilts. A clear power-law dependence of the spatial correlations as a function of pair distance is evident.

We describe the system under study as a set of  $N$  single transverse and longitudinal mode class  $B$  lasers that are coupled linearly to each other through their optical fields. The  $N$  equations for the slowly varying complex electric fields  $E_i$  and the  $N$  equations for the corresponding gains  $G_i$  are

$$\frac{dE_i}{dt} = \tau_c^{-1} \left( (G_i - \alpha_i) E_i - \sum_{j=1, j \neq i}^N \kappa_{ij} E_j \right) + i\omega_i E_i, \quad (2)$$

$$\frac{dG_i}{dt} = \tau_f^{-1} (p_i - G_i - G_i |E_i|^2), \quad (3)$$

where  $\tau_c$  is the cavity round-trip time and  $\tau_f$  is the fluorescence time of the upper lasing level of the Nd:YAG for the  $1064 \text{ nm}$  transition.  $p_i$  and  $\alpha_i$  are the pump and cavity loss coefficients of laser  $i$ , respectively.  $\omega_i$  is the angular

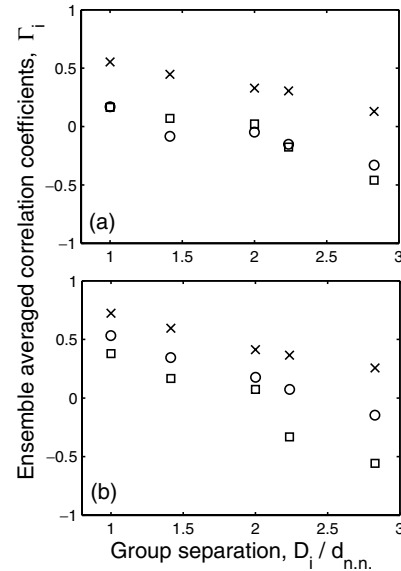


FIG. 2. (a) Experimentally measured ensemble-averaged cross-correlation coefficient  $\langle \Gamma_i \rangle$  as a function of the relative group separation  $D_i/d_{\text{n.n.}}$  in the case of a nine laser array. The three sets of data are related to slightly different tilts of the lens array. (b) Numerically calculated  $\langle \Gamma_i \rangle$  versus  $D_i/d_{\text{n.n.}}$  in the case of a nine laser array. The angular detuning frequencies are chosen from a normal random distribution with mean zero and standard deviation of  $\Delta\omega_c = 2 \times 10^5 \text{ s}^{-1}$  (squares),  $3 \times 10^5 \text{ s}^{-1}$  (circles), and  $2.5 \times 2\pi \times 10^5 \text{ s}^{-1}$  (crosses). They are generated by the *randn* MATLAB function. The state of the generator is set to 1. The corresponding values of  $d_{\text{n.n.}}$  are  $545$ ,  $535$ , and  $485 \mu\text{m}$ , respectively.

detuning frequency of laser  $i$  from a common cavity mode.  $\kappa_{ij}$ , the coupling strength between lasers  $i$  and  $j$ , is taken to be proportional to the overlap of the cavity mode of laser  $i$  with the reflected beam of laser  $j$ , and reads

$$\kappa_{ij} = 2r \frac{w_i v_j}{w_i^2 + v_j^2} \exp\left(-\frac{d_{ij}^2}{w_i^2 + v_j^2}\right), \quad (4)$$

where  $w_i$  is the average  $1/e^2$  beam radius of the Gaussian intensity profile of the cavity mode of laser  $i$  in the crystal while  $v_j$  is the average beam radius of the reflected beam of laser  $j$ .  $r$  is the reflection coefficient of the microlens array and  $d_{ij}$  is the distance between lasers  $i$  and  $j$ . The coupling strength is normalized such that  $\kappa_{ij} = 1$  when  $d_{ij} = 0$ ,  $r = 1$ , and  $w_i = v_j$ . For simplicity, we assume the coupling strengths real and positive. Although this simplification is significant, the model allows one to reproduce the experimental results. In the numerical simulations, we use parameter values that are in agreement with the experiment, namely  $\tau_c = 200$  ps,  $\tau_f = 240$   $\mu$ s,  $p_i = 0.02$ ,  $r = 0.21$ ,  $\alpha_i = 0.01$ ,  $w_i = 105$   $\mu$ m, and  $v_j = 143$   $\mu$ m, and that we assume to be identical for all the elements of the array, the frequency detuning excepted. In the following, we consider Gaussian frequency detuning distributions in the laser array. Randomly chosen detunings with different standard deviations are used to mimic the experimental variation of the orientation of the lens array. In the absence of detuning, the power emitted by each laser is stationary while, in the presence of detuning, the lasers can be driven unstable depending on the coupling or equivalently the nearest-neighbor separation,  $d_{n.n.}$  [11]. If the separation is too large, the interaction between the lasers is so weak that their phases are completely unlocked. By contrast, if the coupling is too strong, then the powers emitted by the lasers are again constant, but this time the phases are perfectly locked. At this point, it is important to note that although each laser is coupled to all the others in Eq. (2) the coupling strength between two nearest-neighbor pairs is larger by at least 2 orders of magnitude than the coupling strength between more distant lasers. In other words, the coupling is effectively local [12]. The individual coupled lasers display chaotic dynamics for the parameter values used.

Figure 2(b) displays the spatial cross-correlation coefficients  $\langle \Gamma_i \rangle$  as a function of the relative pair distances ( $D_i/d_{n.n.}$ ) for three different standard deviations of detuning frequency distributions, namely,  $\Delta\omega_c = 2 \times 10^5$  s $^{-1}$ ,  $3 \times 10^5$  s $^{-1}$ , and  $(2.5 \times 2\pi \times 10^5)$  s $^{-1}$ . The corresponding nearest-neighbor separations were chosen so that the coupling is slightly less than that necessary to achieve phase locking ( $d_{n.n.} < 421$   $\mu$ m for phase locking) and so that the lasers are in a chaotic regime. The spatial cross-correlation coefficient  $\Gamma_i$  is ensemble averaged by computing five time series of 2  $\mu$ s each from different sets of randomly chosen initial conditions. The figure reveals that, for the set of parameters considered here,

the ensemble-averaged cross-correlation coefficients decrease steadily with increasing relative distance between laser pairs, ( $D_i/d_{n.n.}$ ). From multiple numerical simulations, it appears that only positive correlations are observed when the standard deviation of the frequency detuning distribution is large [crosses in Fig. 2(b)]. By contrast, negative correlations can generally be found only when the standard deviation is small enough [squares in Fig. 2(b)]. Comparing Figs. 2(a) and 2(b) shows that the model can predict a behavior of  $\langle \Gamma_i \rangle$  very similar to that experimentally observed.

We are now interested in the dependence of the ensemble-averaged spatial correlations as a function of the nearest-neighbor separation,  $d_{n.n.}$ , the random distribution of the detuning over the laser array being kept constant. Intensive numerical simulations reveal that the obtained results are qualitatively the same regardless of the number of elements in the array. The results are also robust with respect to mismatches of laser parameters and still valid in the absence of several elements of the array. Indeed, we observe a clear power-law dependence of  $\langle \Gamma_i \rangle$  on the relative pair distance, as already suggested by Figs. 2(a) and 2(b) for the nine-element array. In order to substantiate this behavior and to minimize the unavoidable edge effects (the lasers on the edges interacting with fewer neighbors), we consider below a rather large array of 400 lasers ( $20 \times 20$ ). Here, the standard deviation of the angular detuning frequency random distribution over the array is chosen to be  $(2\pi \times 2.5 \times 10^5)$  s $^{-1}$ .

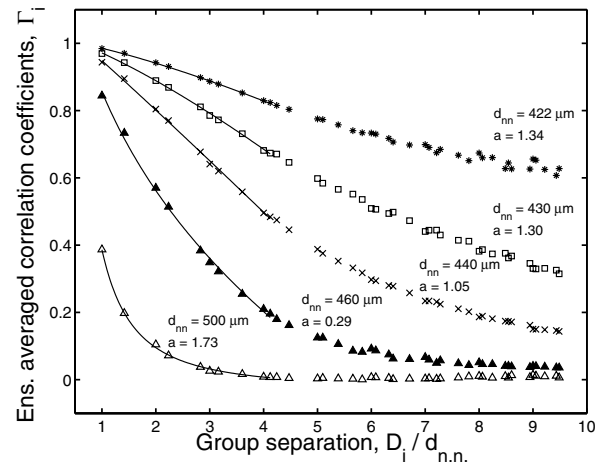


FIG. 3. Numerically calculated ensemble-averaged cross-correlation coefficient  $\langle \Gamma_i \rangle$  as a function of the relative group separation  $D_i/d_{n.n.}$  in the case of a 400 laser array for five different values of the nearest-neighbor separation  $d_{n.n.}$ , namely, 500  $\mu$ m (open triangles), 460  $\mu$ m (filled triangles), 440  $\mu$ m (crosses), 430  $\mu$ m (squares), and 422  $\mu$ m (stars). The distribution of the angular detuning frequencies is generated in the same way as in Fig. 2(b) but with a standard deviation  $\Delta\omega_c = 2.5 \times 2\pi \times 10^5$  s $^{-1}$ . The first ten data points of each distribution have been approximated with the power law  $\langle \Gamma_i \rangle = c - b(D_i/d_{n.n.})^a$ . The corresponding values of the exponent  $a$  are given in the figure.

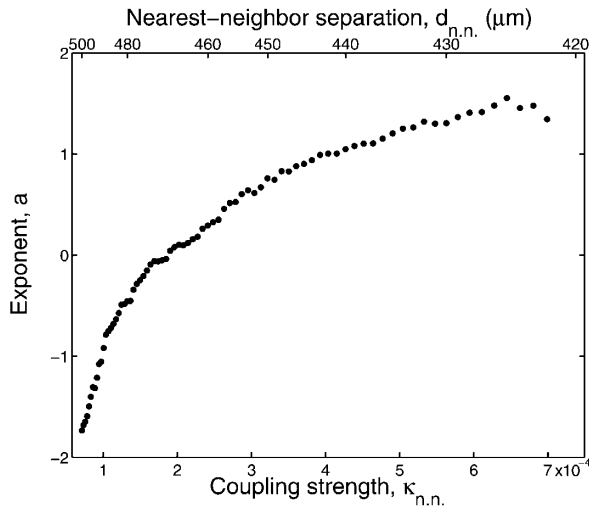


FIG. 4. Numerically calculated exponent  $a$  as a function of the coupling strength and the distance between the nearest-neighbor lasers.

As a consequence, the frequency difference between many nearest-neighbor pairs is of the order of the relaxation oscillation frequency of the solitary lasers. Figure 3 displays the numerically computed  $\langle \Gamma_i \rangle$  as a function of the relative distance between laser pairs ( $D_i/d_{n,n.}$ ) for different values of the nearest-neighbor separation  $d_{n,n.}$ , for which the system operates in a chaotic regime. For rather large separation, the spatial correlation beyond the neighbors is strongly damped revealing the lack of any appreciable synchronization across the array. As  $d_{n,n.}$  decreases, the correlation between nearest neighbors increases rapidly; at the same time  $\langle \Gamma_i \rangle$  rolls off less and less steeply with increasing relative distances ( $D_i/d_{n,n.}$ ). The correlation coefficients presented in Fig. 3 suggest a clear power-law dependence of the ensemble-averaged cross-correlation coefficients of the form  $\langle \Gamma_i \rangle = c - b(D_i/d_{n,n.})^a$  over a spatial range much larger than the coupling. The least-squares approximations related to the numerically calculated coefficients where the  $c$  parameter was optimized to minimize the approximation error are also presented in Fig. 3. The figure shows excellent agreement between the power-law approximations and the numerical computations of  $\langle \Gamma_i \rangle$  with the exponent  $a$  varying continuously with  $d_{n,n.}$ , which is characteristic of the transition from cusp-peaked to flat correlation distributions, as already observed by Kuramoto and Nakao for a large population of identical, nonlocally coupled, chaotic oscillators [6,7]. The behavior of the correlation exponent  $a$  with respect to the coupling strength and, equivalently, the distance between nearest-neighbor lasers is displayed in Fig. 4. The exponent is

observed to vary continuously with the coupling strength, which is again in agreement with the theory developed in Refs. [6,7]. Finally, we also found from numerical simulations that the origin of the power-law dependence is related to the large ratio of time scales (approximately  $10^6$ ) for the fluorescence and cavity lifetimes, as for our experiments. The range of coupling strengths for observation of the power-law becomes significantly smaller as this ratio decreases.

In summary, we have investigated both experimentally and theoretically the behavior of the spatial cross-correlation coefficients in arrays of locally coupled, nonidentical, class  $B$  lasers and demonstrated that they obey a power law with respect to relative laser separation. These new results lead us to expect that previous theoretical predictions by Kuramoto and Nakao [6,7] are not restricted to large sets of chaotic, identical, nonlocally coupled oscillators but can be generalized to a much broader class of dynamical systems.

We acknowledge support from the Physics Division of the Office for Naval Research. F.R. acknowledges the support from the Fonds National de la Recherche Scientifique and the Interuniversity Attraction Pole program 5-18 of the Belgian government. R.R. thanks Steve Strogatz for early discussions and for bringing Refs. [6,7] to his notice.

---

\*Corresponding author.

Electronic address: rogifter@telecom.fpms.ac.be

- [1] K. Kaneko, *Chaos* **2**, 279 (1992).
- [2] A. T. Winfree, *Science* **298**, 2336 (2002).
- [3] A. T. Winfree, *J. Theor. Biol.* **16**, 15 (1967).
- [4] Y. Kuramoto, *Chemical Oscillations, Waves and Turbulence* (Springer, Berlin, 1984).
- [5] I. Z. Kiss, Y. Zhai, and J. L. Hudson, *Science* **296**, 1676 (2002).
- [6] Y. Kuramoto and H. Nakao, *Phys. Rev. Lett.* **76**, 4352 (1996).
- [7] Y. Kuramoto and H. Nakao, *Physica (Amsterdam)* **103D**, 294 (1997).
- [8] Z. Jiang and M. McCall, *J. Opt. Soc. Am. B* **10**, 155 (1993).
- [9] S. Yu. Kourtchatov, V. V. Likhanskii, A. P. Napartovich, F. T. Arcacchi, and A. Lapucci, *Phys. Rev. A* **52**, 4089 (1995).
- [10] R. A. Oliva and S. H. Strogatz, *Int. J. Bifurcation Chaos Appl. Sci. Eng.* **11**, 2359 (2001).
- [11] K. S. Thornburg, M. Möller, R. Roy, T. W. Carr, R.-D. Li, and T. Erneux, *Phys. Rev. E* **55**, 3865 (1997).
- [12] Numerical simulations show that a model with coupling only between nearest-neighbor lasers predicts the same results from Eqs. (2) and (3) as reported here.